View metadata, citation and similar papers at core.ac.uk
brought to you by CORE
provided by HAL-INSU

A contribution to the synsedimentary versus epigenetic origin of the Cu mineralizations hosted by terminal Neoproterozoic to Cambrian formations of the Bou Azzer–El Graara inlier: New insights from the Jbel Laassel deposit (Anti Atlas, Morocco)

Hugo Bourque, Luc Barbanson, Stanislas Sizaret, Yannick Branquet, Claire Ramboz, A. Ennaciri, M. El Ghorfi, L. Badra

To cite this version:

Hugo Bourque, Luc Barbanson, Stanislas Sizaret, Yannick Branquet, Claire Ramboz, et al.. A contribution to the synsedimentary versus epigenetic origin of the Cu mineralizations hosted by terminal Neoproterozoic to Cambrian formations of the Bou Azzer–El Graara inlier: New insights from the Jbel Laassel deposit (Anti Atlas, Morocco). Journal of African Earth Sciences, Elsevier, 2015, 107, pp.108-118. <10.1016/j.jafrearsci.2015.04.005>. <insu-01145561>

HAL Id: insu-01145561
https://hal-insu.archives-ouvertes.fr/insu-01145561

Submitted on 12 Jun 2015

HAL is a multi-disciplinary open access archive for the deposit and dissemination of scientific research documents, whether they are published or not. The documents may come from teaching and research institutions in France or abroad, or from public or private research centers.

L’archive ouverte pluridisciplinaire **HAL**, est destinée au dépôt et à la diffusion de documents scientifiques de niveau recherche, publiés ou non, émanant des établissements d’enseignement et de recherche français ou étrangers, des laboratoires publics ou privés.

Accepted Manuscript

A contribution to the synsedimentary versus epigenic origin of the Cu mineralizations hosted by terminal Neoproterozoic to Cambrian formations of the Bou Azzer – El Graara inlier: new insights from the Jbel Laassel deposit (Anti Atlas, Morocco)

H. Bourque, L. Barbanson, S. Sizaret, Y. Branquet, C. Ramboz, A. Ennaciri, M. El Ghorfi, L. Badra

PII: S1464-343X(15)00078-3
DOI: http://dx.doi.org/10.1016/j.jafrearsci.2015.04.005
Reference: AES 2252

To appear in: *African Earth Sciences*

Received Date: 6 October 2014
Revised Date: 3 April 2015
Accepted Date: 4 April 2015

Please cite this article as: Bourque, H., Barbanson, L., Sizaret, S., Branquet, Y., Ramboz, C., Ennaciri, A., El Ghorfi, M., Badra, L., A contribution to the synsedimentary versus epigenic origin of the Cu mineralizations hosted by terminal Neoproterozoic to Cambrian formations of the Bou Azzer – El Graara inlier: new insights from the Jbel Laassel deposit (Anti Atlas, Morocco), *African Earth Sciences* (2015), doi: http://dx.doi.org/10.1016/j.jafrearsci.2015.04.005

This is a PDF file of an unedited manuscript that has been accepted for publication. As a service to our customers we are providing this early version of the manuscript. The manuscript will undergo copyediting, typesetting, and review of the resulting proof before it is published in its final form. Please note that during the production process errors may be discovered which could affect the content, and all legal disclaimers that apply to the journal pertain.

ACCEPTED MANUSCRIPT

A contribution to the synsedimentary versus epigenic origin of the Cu mineralizations hosted by terminal Neoproterozoic to Cambrian formations of the Bou Azzer – El Graara inlier: new insights from the Jbel Laassel deposit (Anti Atlas, Morocco).

H. Bourque (1)*, L. Barbanson (1), S. Sizaret (1), Y. Branquet (1), C. Ramboz (1), A. Ennaciri (2), M. El Ghorfi (3) and L. Badra (4)

(1)Institut des Sciences de la Terre d'Orléans (ISTO), UMR 7327-CNRS/Université d'Orléans/BRGM, Orléans, France

(2) Managem Group, Casablanca, Morocco

(3) Faculté des Sciences et Techniques – Guéliz, Bd. Abdelkrim El Khattabi - B.P. 549– Marrakech, Morocco

(4 Université Moulay Ismaïl, Meknès, Morocco

* Correspondence to:

hugo.bourque@cnrs-orleans.fr

Institut des Sciences de la Terre d'Orléans
UMR 7327-CNRS/Université d'Orléans
1A rue de la Ferollerie
45071 Orléans Cedex 2
France

T : +33 (0)2 38 49 27 64

ACCEPTED MANUSCRIPT

Abstract

The Neoproterozoic to Cambrian formations that compose the cover of the Bou Azzer-El Graara inlier, host a great number of Copper occurrence whose origin is largely discussed. To bring some light to this debate, structural, petrographic and geochemical observations were performed on the copper deposit of Jbel Laassel. This deposit, located at the extreme ESE of the Bou Azzer –El Graara inlier, is mined since 2012. At the district scale, the ore bodies localize in a folding band that extends along a NE-SW direction. At macroscopic, microscopic and scanning electron microscope scales the mineralization appears as banding veins, with locally cockade breccia and comb quartz textures. From the macroscopic scale to the scale of the scanning electron microscope, all these mineralized textures are connected there between forming a stockwork with an auto-similar structure in the range of used scales of observation. At the district scale, this stockwork is preferentially located in the anticlinal hinges of the folding band. Principal component analyses of geochemical database enable to distinguish several groups of chemical elements, each of these groups corresponding to the different lithologies and to the copper mineralization. This last group doesn't show any correlation with the distinguished lithological groups. All these observations bring new arguments to an epigenetic origin for the copper mineralization of the Jbel Laassel deposit, with a formation contemporary or posterior with the folding band development attributed to Variscan deformation.

Keywords: Anti-Atlas, Cu-mineralization, folding band, stockwork, epigenetic.

1. Introduction

More than 200 Copper mineralizations are known over a large part of the Neoproterozoic to Cambrian cover in the Anti-Atlas (fig. 1A) (Bouchta et al., 1977). They are localized at different stratigraphic levels within the cover and present different characteristics. Their origin remains in most

ACCEPTED MANUSCRIPT

ACCEPTED MANUSCRIPT

cases currently poorly understood and there is no general model for this copper mineralization. Several genetic interpretations have been proposed on specific deposits: (i) based on textural and petrological observations, Leblanc (1986) suggests that Alous mineralization crystallized during the cooling of an ignimbrite; (ii) For the Cu-occurrences of Tizert, Talat N'Ouamane, Tizirt and Amadouz, Pouit (1966), Bouchta & al (1977) and Skacel (1993) consider these mineralizations generated through a synsedimentary process arguing of a strong paleogeographic control of the ores. Moreover, the Cu-mineralizations hosted in the Neoproterozoic to Cambrian cover in the Anti-Atlas can be differentiate by their morphologies as veins, dissemination or stratiform bodies, without relationship have been established between these morphologies yet (Pouit, 1966; Skacel, 1993). As the result, the syngenetic or epigenetic nature of that mineralization remains still undetermined (Pouit, 1966). New data and evidences are then necessary. The Jbel Laassel deposit is one of these numerous cover-hosted copper occurrences known in the Anti-Atlas terminal Neoproterozoic to Cambrian cover, often called Adoudounian cover (Pouit, 1966; Bouchta et al., 1977; Benssaou & Hamouni, 1999). Since the 60's, various genetic models were proposed by several geologists hired by Managem Goup for the copper mineralization at Jbel Laassel site. Maacha et al. (2011) resumed these different models: in 1964 the mineralization was attributed to a porphyry copper type, in 1967 it was interpreted as a stratiform synsedimentary deposit, with a re-concentration stage associated to a Jurassic doleritic intrusion, in 1978 an epigenetic origin was proposed for this mineralization with a mainly vein-shaped texture and a close association with barite. Some authors evoked a synsedimentary genesis for the Jbel Laassel deposit, where mineralization is controlled by the basement paleogeography and were locally remobilized by a tectonic event (Pouit, 1966; Bouchta et al., 1977). According to Skacel (1993), copper should be synchronous with sedimentation; its precipitation being regulated by the redox conditions, themselves under the control on the deposition environment.

In 1984, the MANAGEM Group discovered the potential of the Jbel Laassel Cu-mineralizations. Different preliminary estimations were performed until 2006 (Maacha et al., 2011). In 2010 Managem decided to lead a core drill campaign to estimate the feasibility of this deposit. This work resulted in an estimation of 7.5 million tons at 1% Cu (Maacha et al., 2011) and the exploitation

ACCEPTED MANUSCRIPT

began in 2012 with SOMIFER as operator. In this article, based on MANAGEM Group pre-exploitation targeting, we report the main results of an original study performed on Jbel Laassel Cu-mineralization. This work consists of: (i) a structural analysis of ore bodies, (ii) a mineralogical study of samples collected both on outcrops and drill cores and (iii) a statistical analysis of the first chemical analyses carried out in this deposit. These new data bring out new insights on the debated, epigenic versus syngenetic origin of the Jbel Laassel deposit.

2. Geological setting

2.1. The Bou Azzer El Graara inlier

The Bou Azzer El Graara inlier is one of a series of Proterozoïc windows oriented NW-SE that expose Panafrican formations in the central part of the Anti-Atlas (Choubert, 1947). The Proterozoic basement is mainly composed by a dismembered ophiolitic sequence and arc fragments (Leblanc, 1975; Saquaque et al., 1989) (fig. 1B). These formations are uncomformably overlain by a thick Neoproterozoïc to Cambrian volcano-sedimentary cover (Soulaimani et al., 2014). This cover can be divided into three formations from bottom to top: (1) The Tiddiline Formation (~750 to 650 Ma) attributed to the “Saghro Group” (Thomas et al. 2004), composed of clastic, volcanoclastic and volcanic series, rests mainly uncomfortably on the Panafrican substratum; (2) The Ouarzazate Group (~610 to 550 Ma), composed of a volcano sedimentary complex, rests in angular unconformity on the Tidiline Formation; (3) Terminal Neoproterozoïc to Cambrian Formations consisting of detrital and carbonated series (Soulaimani et al., 2013). These Terminal Neoproterozoïc to Cambrian Formations, varying in age from terminal Neoproterozoïc to the middle Cambrian, are associated with a major marine transgression toward the Southeast and can be subdivide into two groups: the Taroudannt Group and the Tata Group (fig. 2). During the Late Paleozoic compressional event, the Panafrican structures of the basement were reactivated along the inlier’s borders. This results in box-shaped folds distributed throughout the Bou Azzer-El Graara area and by large open synclines of Cambrian rocks (Soulaimani & Burkhard, 2008). Upright detachment folds, from meters to decameters in scale, are

ACCEPTED MANUSCRIPT

ACCEPTED MANUSCRIPT

frequent in the lower Cambrian rocks and they exhibit a dominant NW-SE trend with subordinate NE-SW structures (Soulaimani & Burkhard, 2008).

2.2. Lithostratigraphy of the Jbel Laassel Cu-deposit

The Jbel Laassel deposit is hosted in the Lower Cambrian part of the Neoproterozoïc to Cambrian volcano-sedimentary cover, at the extreme ESE part of the Bou Azzer-El Graara inlier, 30 kilometers NE of the Bleida mine (fig. 1B). The whole of this cover is often call Adoudounian cover, it is a local appellation, and on the other hand the term Adoudou correspond to the name of a precise stratigraphic formation (Soulaimani et al, 2013). The Lower Cambrian is represented in the studied site by the Adoudou and Tikirt Formations, both belonging to the Taroudann Group, whereas the Igoudine, Amouslek, Issafene and Tazlaft Formations correspond to the Tata Group (fig. 2) (Soulaimani et al., 2013). All these formations are interlayered locally with volcanic flows dated at 534 ± 10 Ma (U/Pb on zircon by Ducrot & Lancelot, 1977) related to the Jbel Boho-type volcanism (Alvaro et al., 2006) (fig. 1 and 2).

2.2.1 The Taroudannt Group

The Adoudou Formation (Choubert, 1952) is represented in the area study by a basal sedimentary breccia with a thickness of 5 to 100 meter and by an alternation of dolostones and red or white clay’s siltstones with a total thickness varying from 150 to 250 meters. Dolostones frequently present an intensive secondary silicification (Soulaimani et al., 2013). The Tikirt Formation (250 to 300 meters thick) rests in conformity on the Adoudou Formation; it is composed essentially by sandstones frequently interlayered by centimetric clayed siltstones. The age of this formation is unknown; but the Taliwine Formation, a westward stratigraphic equivalent level has been dated by U/Pb on zircon from Early Cambrian volcanic horizons at 521 ± 7 Ma and 522 ± 2 Ma (Compston et al., 1992; Landing, 1998; Maloof et al., 2005). On the Jbel Laassel site and at regional scale, Tikirt sandstones end with a continuous level of red claystones 8 to 15 meters thick (fig. 2).

ACCEPTED MANUSCRIPT

ACCEPTED MANUSCRIPT

2.2.2 The Tata Group

This Group includes, from oldest to youngest, the formations of Igoudine, Amouslek, Issafène and Tazlaft. The age of the Tata Group varies from the Tomotien (in the lower Cambrian) at its base, to the Middle Cambrian at its top. (Soulaimani et al., 2013). The Igoudine Formation (50 to 60 meters thick) is made up of dolostones with microbialite interlayered with clayed siltstones or siltstones. The Amouslek Formation appears as an alternation of stromatolitic dolostones with heterolitic facies of clayed siltstones, for a total thickness of 150 to 180 meters. The Issafene Formation is composed by red claystones and thin beds of sandstones, and it is 30 to 40 m thick (Soulaimani et al., 2013). The Tazlaft Formation, 90 to 100 meters thick, is composed of sandstones with oblique cross bedding and mega-ripples marks (Soulaimani et al., 2013).

3. Methodology and Analytical procedure

In order to decipher the complex pattern of geometries and structures, a structural study has been performed in the field coupled with high density drill control. As a result, well constrained and high resolution maps and cross-sections have been constructed (fig. 3 to 5).

During the field work, 10 samples have been collected from outcrops and 55 samples have been collected on 9 core drills. 60 polished thin sections were prepared from these samples. They have been first observed using a Leica DMRX petrographic microscope (transmitted and reflected light modes). Complementary observations and analyses were carried out using JSM-6400 JEOL Scanning Electron Microscope (SEM) at ISTO. Polished thin-sections have been first coated by a thin carbon layer. Acceleration voltage and beam current were 20 kV and 8 nA, respectively. IdFix Software package was used for data processing. Back-scattered electrons (BSE) imaging mode was used to reveal the composition variations at microscopic scale, whereas the texture of clayey material was examined with secondary electrons (SE) imaging mode. The SEM system is coupled to an Energy-Dispersive X-ray spectrometer (EDS) to make qualitative determinations of the mineral composition.

ACCEPTED MANUSCRIPT

ACCEPTED MANUSCRIPT

The Managem Group performed analyses on 23 Reverse Circulation drilling's samples collected at different depths for the following elements: Cu, CuOx, SiO_2, Al_2O_3, Fe_2O_3, CaO, MgO, K_2O, MnO, TiO_2, P_2O_5, As, B, Ba, Be, Bi, Cd, Co, Cr, Ge, Li, Mo, Nb, Ni, Pb, Sb, Se, Sn, Sr, W, Y, Zn, Ag and loss on ignition (LOI). "Cu" corresponds to the total copper content and CuOx corresponds to the non-sulphide copper content. For the major elements analysis, 0.5 g of the sample is crushed at less than 100µm and it is dissolved by fusion at 500°C during 45 minutes with 2.5 g of sodium peroxide in a zirconium crucible. The melt mixing is dissolve with 100 ml of hydrochloric acid (28% HCl) and the solution is analyzed using an ICP-AES ULTIMA 2C using the Jobin Yvon-HORIBA device. For the other elements, 0.25 g of the sample is dissolved by acid attack (50%HCl and 50% HNO_3) microwave-assisted during 45 minutes at 220°C. The solution is then analyzed by ICP-MS Thermo X'Serie 2.

4. Results

4.1. Structural study

The whole sequence undergoes at least one deformation stage. Two types of folds are present. The first family corresponds to upright folds characterized by sub-horizontal to slightly NW dipping axes with a NW-SE to NNW-SSE orientation (fig. 3b). They are marked by an axial planar cleavage particularly developed in the fold hinge zone. Those NW-trending folds are concentrated in a band, named herebelow "folding band", which displays a width of 150 to 200 meters and is oriented N145° (fig. 3 and 4). This "folding band" is developed along a N150E-trending vertical fault, folds being localized in both sides of the fault. The second fold family shows moderately inclined fold's axes to the NE, oriented NE-SW (fig. 3). The orientation of NE-trending folds is parallel to the direction (around N30°) of a SE-vergent thrust that outcrops through the entire area (fig. 3). Therefore, at large scale, the Jbel Laassel area and its ore body appears to be located within a large NE-trending synclinal developed in the thrust footwall (figure 3). The relations between the two types of folds could not be observed in the field. In the thrust hanging wall, a similar vertical fault is found northeastward (fig. 3) with sub-parallel folds and mineralizations along the northwestern prolongation (out of fig. 3).

ACCEPTED MANUSCRIPT

Consequently, we infer that both hanging- and footwall vertical fault segments are part of the same vertical fault offset by the late thrust. As the fault is vertical, the thrust might have right lateral oblique slip component of about 300 meters.

4.2. Jbel Laassel ore bodies

4.2.1. Geometries and orientation

The vertical and lateral extent of ore bodies was delimited by surface cartography and drills. Part of the outcrops are covered by superficial alteration formations and mining waste. Ore bodies extend 150 to 250 meters in width (fig. 4), with a maximal longitudinal extension of 400 meters (fig. 3) for an average thickness of around 100 meters (fig. 4 and 6). Mineralization is hosted in Igoudine and Amouslek Formations and more especially in dolostones and siltstones beds, rarely in lavas or claystones beds. It is noteworthy that ore bodies are distributed within and along the "folding band" with an orientation NE-SW i.e., they show the same preferential orientation as that of the folds (fig. 3). Moreover, on a NE-SW cross section (fig. 4), the ore bodies show thickness variation: in the hinge of anticlinal the thickness is maximal whereas in the hinge of synclinal the thickness is minimal (fig. 4). Similarly, the vertical fault strongly controls the ore bodies distribution with a nearly barren southwestern compartment contrasting with a rich folded northeastern one (fig. 4). On a NW-SE cross section, the thickness of the ore bodies is constant and does not show significant variation (fig. 5).

4.2.2 Mineralogical composition and paragenetic succession

Without distinction between primary and secondary origin, the copper mineralization is composed of chalcocite, bornite, chalcopyrite, covellite, digenite, malachite, chrysocolla, tenorite, native copper and cuprite, associated with quartz, dolomite and calcite as gangue mineral. These gangue minerals in veinlets or voids systematically show, a banding texture. The observed growth direction indicates a centripetal quartz, dolomite and finally calcite (fig. 6A). This gangue chronology

ACCEPTED MANUSCRIPT

ACCEPTED MANUSCRIPT

is a good landmark to determine the copper mineral succession. Bornite appears as minute grains (less than 20 µm) in the quartz and dolomite ribbons, equally distributed between these two minerals. Frequently, lamella exsolutions of chalcopyrite are observed in bornite grains. Chalcocite occurs in ribbon between the bands of dolomite and calcite. Chalcocite grains mostly appear with an anhedral shape without internal structure. Sometimes this mineral displays a hexagonal cleavage (fig. 6B and 6C), suggesting, in this case, a primary origin at above 103°C (Ramdhor, 1969). This generation of chalcocite is named CC1. Beside, chalcocite exists in association with covellite, digenite and chalcopyrite, in replacement around the bornite, in this case chalcocite, covellite and digenite can be interpreted as cementation assemblage. This chalcocite is named CC2. Malachite replaces chalcocite and dolomite and may be replaced by chrysocolla. Malachite also replaces cuprite but sometimes the opposite situation is observed. Veinlet fills only by malachite are been observed, they cut all the other rock components and structures except chrysocolla.

All these relations between minerals allow to discriminate a primary origin represented by: quartz, bornite, chalcopyrite, dolomite, chalcocite (CC1) and calcite, and a secondary origin represented by: covellite, digenite, chalcocite (CC2), malachite, chrysocolla, tenorite, native copper and cuprite (fig. 7). Based on intersections relations between the different mineral phases, several episodes of fissuring have been observed (fig. 7).

4.2.3 Multiscale observations of the ore texture

At macroscopic scale, on core samples, two textural types of mineralization have been distinguished. The most frequent is a stockwork with veins/veinlets parallel or oblique to the stratification plane (fig. 8). Parallel-bedding veins are still connected to cross-bedding veins (fig. 8C). The second type corresponds to disseminations within the rock ground mass. Locally it is spatially related to the stockwork (fig. 8D). When it is well develop, veins of the stockwork can show breccia texture with angular fragments and in situ fragmentation texture without significant rotation of the fragment that is characteristic of fluid-assisted brecciation (Jébrak, 1997) (fig. 8A). At the microscopic scale, both types of mineralization appear composed by the same ore and gangue minerals. Textural

ACCEPTED MANUSCRIPT

and chronological relationships being also similar, both mineralization types have the same paragenetic sequence (fig. 6, 7 and 8). Veins can also locally show a cockade breccia and quartz with comb texture (fig. 6F and 6G). At this scale, disseminated grains of copper-bearing minerals, down to 50 micrometers in size, are still observable (fig. 6E). Noteworthy, they frequently show a close spatial relationship with the veinlet of the stockwork (fig. 6E). At the scanning electron microscope scale, the disseminated mineralization appears as micro-voids or geodes that display the same mineralogical content and the same paragenetic succession as that observed at higher observation scales (i.e. with quartz or dolomite at the wallrock and chalcocite at the center) (fig. 9).

4.2.4 Mineralogical distribution at the deposit scale

Using the data collected on 9 core drills and on surface mapping, the Cu-bearing mineral abundance is plotted in cross-sections (fig. 4 and 5). The mineralogical abundances are displayed in the form of spider diagram, with, at the top, the secondary Cu-bearing "oxydized" minerals (malachite, chrysocolla and cuprite) and at the bottom the primary or cementation Cu-bearing minerals (chalcocite, bornite and chalcopyrite). The mineralogical abundances are evaluated through microscopic observations of polished thin sections of mineralized cores. The content of each mineral is evaluated visually using an abundance chart (Dutro et al., 1989). Results are expressed in the corresponding axis of the spider diagram in a scale of 0 to 100% with steps of 20%.

Chalcocite and malachite are the most abundant minerals in the Jbel Laassel deposit (fig. 4 and 5). According to our observations, no obvious zonation appears between primary sulfides and “oxidized” mineralization.

4.3. Principal Component Analysis (PCA) of chemical data

Two muli-element databases were available for PCA: the larger one, does not include Cu analyses, while the second one includes Cu analyses for a smaller number of samples. PCA analysis was performed on both sets separately using varimax criteria.

ACCEPTED MANUSCRIPT

ACCEPTED MANUSCRIPT

4.3.1. Dataset without copper measurements

The first results on database without copper measurements (228 analyses) show that two factors F1 and F2 explain 42.06 % of the total variability (fig. 10A). Three groups of elements discriminated in the F1-F2 plane represented by the CaO, MgO and MnO cluster (group 1) discriminates he carbonate matrix, the second SiO2, Al2O3, K2O and B clusters represents the clay sedimentary component (group 2) whereas the last Co, P2O5, Fe2O3, TiO2 and Pb cluster (group 3) probably marks the lava component (fig. 10B). Thus, referring to the F1 F2 chemical space (fig. 10C), the analyzed dolostones consists of alternation of siltstones and dolostone layers, with interstratified lavas in both of them. It appears that the three groups of variables can be interpreted in terms of lithology: the groups 1, 2 and 3, corresponding respectively to dolostones, siltstones and lava formations (fig. 10C).

4.3.2 Dataset including copper measurements

This data set comprises 72 analyses. For the Cu-mineralized data set (Cu % and CuOx %), the four first factors account for 80% of the total variance. Beyond factor 4 the explained variance decreases sharply. The plane F1-F2 represents 48.29% of the total variance (28.27% for F1 and 20.01 for F2). The three petrographic groups previously identified in the F1-F2 plane are well discriminated by the same element clusters (fig. 10D). This representation of the variables suggests that copper (total or oxidized) is not linked to any of the three types of lithology. Indeed, copper is independent of sedimentary dolostones and siltstones, and it is anticorrelated with the lavas (fig. 10D). Moreover, an examination of the F1-F2 plane, suggests that copper could be associated with barium, but the correlation coefficient between total copper and barium is -0.05 and that of barium with oxidized copper is 0.03. This is due to the fact that the total copper, oxidized copper and barium are badly represented in the plane F1 - F2, as shown in the diagram in figure 10D and by the values of the weighting coefficients between the original variables and factors. For total copper, oxidized copper and barium, these values are -0.19, -0.23 and -0.16 with respect to F1 and -0.30, -0.38 and -0.38 relative to F2. The factors where copper (total and oxidized) is best represented are F3 and F6. The

ACCEPTED MANUSCRIPT

ACCEPTED MANUSCRIPT

weighting coefficients between the copper, the oxidized copper and the factors are 0.54 and 0.42 with respect to F3 and 0.59 and 0.63 relative to F6, respectively. The variables representation in the plane F3-F6 (17.37% of the total variance, 12.55% for F3 and 4.82% for F6) shows that the variations of the total copper and of the oxidized copper are not associated with changes in the others variables values (fig. 10E). Therefore, the PCA highlights the independence of copper (total and oxidized) relative to the others variables present in the available database, especially that corresponding to lithology.

5. Discussion

In the Jbel Laassel copper deposit, at a macroscopic scale, the mineralization is present as a stockwork and disseminations. The stockwork is composed by veins filled with a primary paragenesis composed by: quartz, bornite, chalcopyrite, dolomite, chalcocite, calcite and a secondary paragenesis composed by: covellite, digenite, malachite, chrysocolla, tenorite, cuprite and native copper. The veins of this stockwork crosscut the stratification plane or are parallel to it. Both vein families always present the same mineralogy, texture and paragenetic evolution. These observations suggest that, with respect to the primary sulfide paragenesis, all the stockwork veins are coeval and formed during the same mineralizing event. SEM observations reveal that disseminations correspond to microcracks and cavities filled with the same mineralogical content and the same textural characteristics that of stockwork veins; moreover the disseminated Cu-bearing mineral grains are directly “connected” to the stockwork veins. Thus, all the primary mineralization, from the macroscopic scale to the scanning electron microscope scale, is related to the stockwork and deposited during a unique hydrothermal event of fluid assisted fracturation of the host sedimentary rocks. All these observations favor an epigenetic origin of the Jbel Laassel mineralization. In addition, the principal component analysis shows that copper does not have affinities with any of the lithological groups present in the area. This result is also consistent with an epigenetic origin of the mineralization. The limits of the ore body correspond to the limits of the “folding band” (fig. 3). In the cross-section perpendicular to the main extension of the folding band (fig. 4), the ore body is concentrated in the anticline hinges and his thickness decreases in syncline hinges; whereas in cross section parallel to the main extension of the folding axis, the ore body is continuous and does not show noticeable thickness variations (fig. 5).

ACCEPTED MANUSCRIPT

ACCEPTED MANUSCRIPT

Consequently the mineralized stockwork is clearly controlled by hectometric folds, which are, with the Igoudine and Amouslek Formations, the trap of the mineralization. Available structural and fault analysis data do not allow us to decipher clearly the control exerted by the vertical faults on NW-trending mineralized folds. However, the structural pattern associated with the "folding band" suggest folding developed within the cover above fault involving basement through drap folding and/or flower structure mechanisms (Sylvester, 1988; Fossen et al., 2013).

Soulaimani & Burkhard (2008) describes variscan kink bands with a rough cleavage in the vicinity of Panafrican structures in the basement of the Bou Azzer El Graara inlier. These authors interpret these folds in terms of the reactivation of Panafrican structures during the late Paleozoic compression. In the terminal Neoproterozoic to Cambrian’s cover, folds are currently attributed to this Paleozoic compression, controlled by the movement of inherited basement structures (Leblanc, 1972; Soulaimani, 1997; Faïk et al, 2002; Soulaimani & Burkhard, 2008). It results in Bou Azzer-El Graara inlier, metric to decametric folds, have NW-SE trending axes exhibit with a subordinate NE-SW orientation (Soulaimani & Burkhard, 2008). The folds in the “folding band” of Jbel Laassel display the same characteristics as the ones given by Soulaimani & Burkhard (2008), for the Variscan folds, i.e. metric to decametric folds and NW-SE trending axes with a subordinate NE-SW orientation. In such conditions, the age of the mineralizing event could probably be contemporary to the deformation or younger. It could be possible that the intersection between the “folding band” and the NE-SW synclinal took a role in the trap of mineralization formation. This “folding band” is associated with a major NW-SE fault with a kilometers extension. This fault probably acted as a drain for fluids that formed the mineralization of the “folding band” in the Jbel Laassel area. Anticlinal hinges of the “folding band” could be a trap for hydrothermal discharges with a fluid-assisted fracturing focused in these hinges. The major NW-SE fault could be in direct relation with the basement, as reported by Soulaimani & Burkhard (2008) for the others Variscan faults in the terminal Neoproterozoic to Cambrian cover. This fault could thus emphasize a basement influence at the origin of the Cu mineralization of Jbel Laassel. We propose that Cu mineralization hosted in the terminal Neoproterozoic to Cambrian cover are linked to Variscan reactivation of inherited basement structures

ACCEPTED MANUSCRIPT

ACCEPTED MANUSCRIPT

and Variscan faults that drained fluids which precipitated its copper content in the anticlinal hinge of the Jbel Laassel "folding band".

9. Conclusion

The copper mineralization in Jbel Laassel area is epigenetic and is controlled and coeval with decametric folding, whose axes exhibit a NW-SE trend in the Igoudine and Amouslek Formations. These folds are concentrated in a 150 to 200 m wide band, probably formed during the Variscan compression. Consequently the mineralizing event took place during this period or later. The mineralization appears as a stockwork, displaying the same characteristics (texture and mineral composition) from the macroscopic scale to the scale of the scanning electron microscope, i.e. it shows a textural autosimilarity regardless the scale. The proposed interpretations therefore should not be extended to the others mineralization hosted in the Neoproterozoic to Cambrian’s cover of the Bou Azzer El Graara inlier without any further study. On the other hand, for academic but also applied purposes, this work highlights the necessity to perform more detailed studies of the Cu-occurrences hosted in the cover of the Bou Azzer El Graara inlier to reevaluate the factors controlling these mineralizations.

Acknowledgment

This work was supported by the research project “CALAMINE” .Fieldwork has been financed by Managem. Thanks are due to M. Jébrak and P. Ericksson for their accurate and constructive reviews. We are also indebted to I. Di Carlo (ISTO), P. Pehnoud (ISTO), N. Pothier (ISTO), J.-G. Badin (ISTO) and S. Janiec (ISTO) for the sample preparation, the assistance for bibliography, analyses and data treatment.

Bibliography

ACCEPTED MANUSCRIPT

ACCEPTED MANUSCRIPT

Alvaro J.J., Ezzouhairi H., Vennin E., Ribeiro M.L., Clausen S., Charif A., Ait Ayad N., Moreira M.E., 2006. The Early-Cambrian Boho volcano of the El Graara massif, Morocco: Petrology, geodynamic setting and coeval sedimentation. J. Afr. Earth Sci. 44, 396-410.

Benssaou M. et Hamouni N., 1999. Paléoenvironnements et minéralisations de l'Anti-Atlas occidental marocain au Cambrien précoce. Chron. Rech. Min. 536-537, 113-119.

Bouchta R., Boyer F., Routhier P., Saadi M. et Salem M., 1977. L'aire cuprifère de l'Anti-Atlas (Maroc); permanence et arêtes riches. C. R. Acad. Sc. Paris 284, 503-506.

Boudda A., Choubert G., Faure-Muret A., 1979. Essai de stratigraphie de la couverture sédimentaire de l'Anti-Atlas : Adoudounien-Cambrien inféieur. Notes et Mémoires du Service Géologique du Maroc. 271, 96 pp.

Choubert G., 1947. L'accident majeur de l'Anti-Atlas. Comptes Rendus de l'Académie des Sciences 224, 1172–1173.

Choubert G., 1952. Histoire géologique du domaine de l'Anti-Atlas. In: Géologie du Maroc. Notes et Mémoires du Service Géologique du Maroc 100, 75–194.

Compston W., Williams J.L., Kirschvink J.L., Zhang Z., Ma G., 1992. Zircon U-Pb ages for the Early Cambrian time scale. Journal of the Geological Society, London 127, 319-332.

Ducrot J., Lancelot J.R., 1977. Problème de la limite Précambrien-Cambrien: étude radiochronologique par la méthode U/Pb sur zircon du volcan du Jbel Boho. Can. J. Earth Sci. 14, 1771-1777.

Dutro, J.T., Dietrich R.V., Foose R.M., 1989. AGI Data Sheets: or geology in the field, laboratory, and office, ed. American Geological Institute, Virginia, U.S.A

ACCEPTED MANUSCRIPT

ACCEPTED MANUSCRIPT

Faik K., Belfoul M.A., Bouabdelli M. et Hassenforder B., 2002. Les structures de la couverture Néoprotérozoïque terminal et Paléozoïque de la région de Tata, Anti-Atlas centre-occidental, Maroc: déformation polyphasée, ou interactions socle/couverture pendant l'orogenèse hercynienne? J. African Earth Sci. 32, 765-776.

Fossen H., Teyssier C., Whitney D. L., 2013. Transtensional folding. J. Struct. Geol. 56, 89-102.

Jébrak M., 1997. Hydrothermal breccias in vein-type ore deposits: A review of mechanisms, morphology and size distribution. Ore Geology Reviews 12, 111-134.

Kersit, 1984. Internal report, Managem, 40 pp.

Landing E., 1998. Cambrian subdivisions and correlations. Can. J. Earth Sci. 35, 4.

Leblanc M., 1972. Sur le style disharmonique des plis hercyniens de la couverture, Anti-Atlas central (Maroc). Comptes Rendus de l'Académie des Sciences 275, 803-806.

Leblanc M., 1975. Ophiolites précambriennes et gîtes arséniés de Cobalt (Bou-Azzer, Maroc). Notes et Mémoires du Service Géologique du Maroc, 280, 306 pp.

Leblanc M., 1986. Appareil ignimbritique et minéralisation cuprifère: Alous (Anti-Atlas, Maroc). Mineral. Deposita 21, 129-136.

Maacha L., Ennaciri A., El Ghorfi M., Baoutoul H., Saquaque A., Soulaimani A., 2011. The J. La'sal Oxidized Copper Deposit (El Graara inlier, Central Anti-Atlas), in: Mouttaqi A., Rjimati. E.C., Maacha L., Michard A., Soulaimani A., Ibouh H. (Eds), New geological and mining guidebook of Morocco. Volume 9. Main Mines of Morocco. Service Géologique du Maroc, Rabat, pp. 117-121.

Maloof A.C., Schrag D.P., Crowley J.L., Bowring S.A., 2005. An expanded record of Early Cambrian carbon cycling from the Anti-Atlas Margin, Morocco. Can. J. Earth Sci. 42, 2195-2216.

ACCEPTED MANUSCRIPT

Pouit G., 1966. Paléogéographie et répartition des minéalisations stratiformes de cuivre dans l'anti atlas occidental (Maroc). Chron. Rech. Min 356, 279-289.

Ramdhor P., 1969. The ore minerals and their intergrowths. Pergamon Press, 117 pp.

Saquaque A., Admou H., Karson J. A., Hefferan, K. & Reuber I., 1989. Precambrian accretionary tectonics in the Bou Azzer–El Graara region, Anti-Atlas, Morocco. Geology 17, 1107–1110.

Sylvester A.G., 1988. Strike-slip faults. Geol. Soc. Am. Bull. 100, 1666-1703.

Skacel J., 1993. Gisement cuprifère polygénétique de Tazalagh (Anti-Atlas occidental). Mine, Géologie & Energie 54, 127-133.

Soulaimani A., Le Corre Cl., Farazdaq R., 1997. Déformation hercynienne et relation socle/couverture dans le domaine du Bas Drâa (Anti-Atlas occidental, Maroc). J. Afr. Earth Sci., 24, 271-284.

Soulaimani A. and Burkhard M. 2008. The Anti-Atlas chain (Morocco): the southern margin of the Variscan belt along the edge of the West African craton. Geological Society of London, Special Publications 297, 433-452.

Soulaimani A., Egal. E., Razin Ph., Youbi N., Admou H., Blein O., Barbanson L., Gasquet D., Bouabdelli M., 2013. Notice explicative de la carte géologique du Maroc au 1/50 000, feuille Al Glo'a. Notes et Mémoires du Serv. Géol. Maroc 532 bis, 140 pp.

Soulaimanie A., Michard A., Ouanaimi H., Baidder L., Raddi Y., Saddiqi O., Rjimai E.C., 2014. Late Ediacaran-Cambrian structures and their reactivation during the Variscan and Alpine cycles in the Anti-Atlas (Morocco). J. Afr. Earth Sci., 98, 94-112.

ACCEPTED MANUSCRIPT

Thomas R.J., Fekkak A., Ennih N., Errami E., Loughlin S.C., Gresse P.G., Chevallier L.P., Liégeois J.-P., 2004. A new lithostratigraphic framework for the Anti-Atlas Orogen, Moocco. J. Afr. Earth Sci. 39, 217-226.

Figures:

Figure 1: A: Schematic geologic map of the Anti-Atlas with occurrences of copper mineralizations modified from Bouchta et al. (1977). Inliers abbreviations : If, Ifni; Kr, Kerdous; Ir, Igherm; TA, Tagragra d'Akka; TT, Tagragra Tata; AM, Agadir Melloul; Ze, Zenaga; Sr, Sirwa; Bz, Bou Azzer-El Graara; Sg, Saghro; Og, Ougnate. **B:** Geological and structural map of the Bou Azzer-El Graara area with occurences of copper mineralizations, modified from Leblanc (1975).

Figure 2 : Lithostratigraphic column for the Jbel Laassel area modified from Soulaimani et al. (2013).

Figure 3: (a) Geological and structural map of the Jbel Laassel area, modified from Kersit (1984); **(b)** Stereogram (Wulff stereonet, lower hemisphere) of bedding (S_0) and fold axes (n, number of measures).

Figure 4: Geological cross-section (section location A-A' in the map) with ore body limits and mineralogical aboundance of the copper mineraliation which are represented in a spider diagram. Results are expressed in the corresponding axis of the spider diagram in a scale of 0 to 100% with steps of 20%. Abbreviations: Mal, malachite; Ccl, chrysocolla; Cup, cuprite; Dg, digenite; Bn, bornite; Ccp, chalcopyrite; Cc, chalcocite.

Figure 5: Geological cross-section (section location B-B' in the map) with ore body limits and mineralogical aboundance of the copper mineralization which are represented in a spider diagram. Results are expressed in the corresponding axis of the spider diagram in a scale of 0 to 100% with steps of 20%.. Same abreviations than fig.5.

Figure 6: Microphotographs of the Jbel Laassel Cu ore. **A:** Vein showing banding gangue texture with quartz on wall, next dolomite and calcite at center (TL nic. +). **B:** Chalcocite in ribbon between

ACCEPTED MANUSCRIPT

bands of dolomite and calcite (RL, nic. //). **C:** Chalcocite in vein with hexagonal cleavage (RL, nic. //). **D:** Quartz and chalcocite veinlet link to a vein forming a stockworck (TL, nic. //). **E.1:** Quartz vein cutting bedding (S0) of siltstone and silicification of the siltstones bedding (TL, nic.//). **E.2:** Same photography as E.1 but in RL (nic. //), chalcocite in vein and in dissemination in silicified bedding, these disseminations were observed at SEM scale (see fig.9). **F:** Quartz, dolomite and chalcocite vein showing micro-cockade breccia texture (TL, nic. //). **G:** Quartz in vein with comb texture and malachite veinlets cutting other rock components and structures (TL, nic. +). Abbreviations: Cc1, primary chalcocite; Dol, dolomite; Mal, Malachite; Qtz, quartz. TL, transmitted light; RL, reflected light; nic. //, parallel nicols; nic. +, crossed nicols; S0, bedding of rock.

Figure 7: Paragenetic succession.

Figure 8: Photographs of core drill samples. **A:** Stockworck with gangue minerals, chalcocite, chrysocolla and malachite, and a fluid assisted breccia texture. **B:** Chalcocite stockwork. **C:** Chalcocite stockworck with vein secant and parallel to the dolostone bedding. **D:** Veins of chalcocite cutting the dolostone beding and chalcocite in dissemination in dolostone but linking to the vein, these disseminations were observed at SEM scale (see fig.9). Abbreviations are given in figure 7.

Figure 9: SEM photographs of disseminated copper mineralization (see figures 6E and 7D). **A:** BSE image of a micro-vein (100 µm width) composed by quartz, dolomite and chalcocite. **B:** BSE image of a micro-vein (25 µm width) composed by quartz, dolomite and chalcocite.

Figure 10: Results of PCA analyses of the data base without copper (A, B and C) and of the data base with copper (D and E). **A:** Eigenvalues and cumulative variance function of factors. **B:** Variables projection in the F1-F2 plane (data set without copper: 228 analysis). **C:** samples lithology project in F1-F2 plane (data set without copper: 228 analysis) and Variables projection in the F1-F2 plane without legends. **D:** Variables projection in the F1-F2 plane (data set including copper: 72 analysis). **E:** Variables projection in the F3-F6 plane (data set including copper: 72 analysis).

ACCEPTED MANUSCRIPT

Figure 1

ACCEPTED MANUSCRIPT

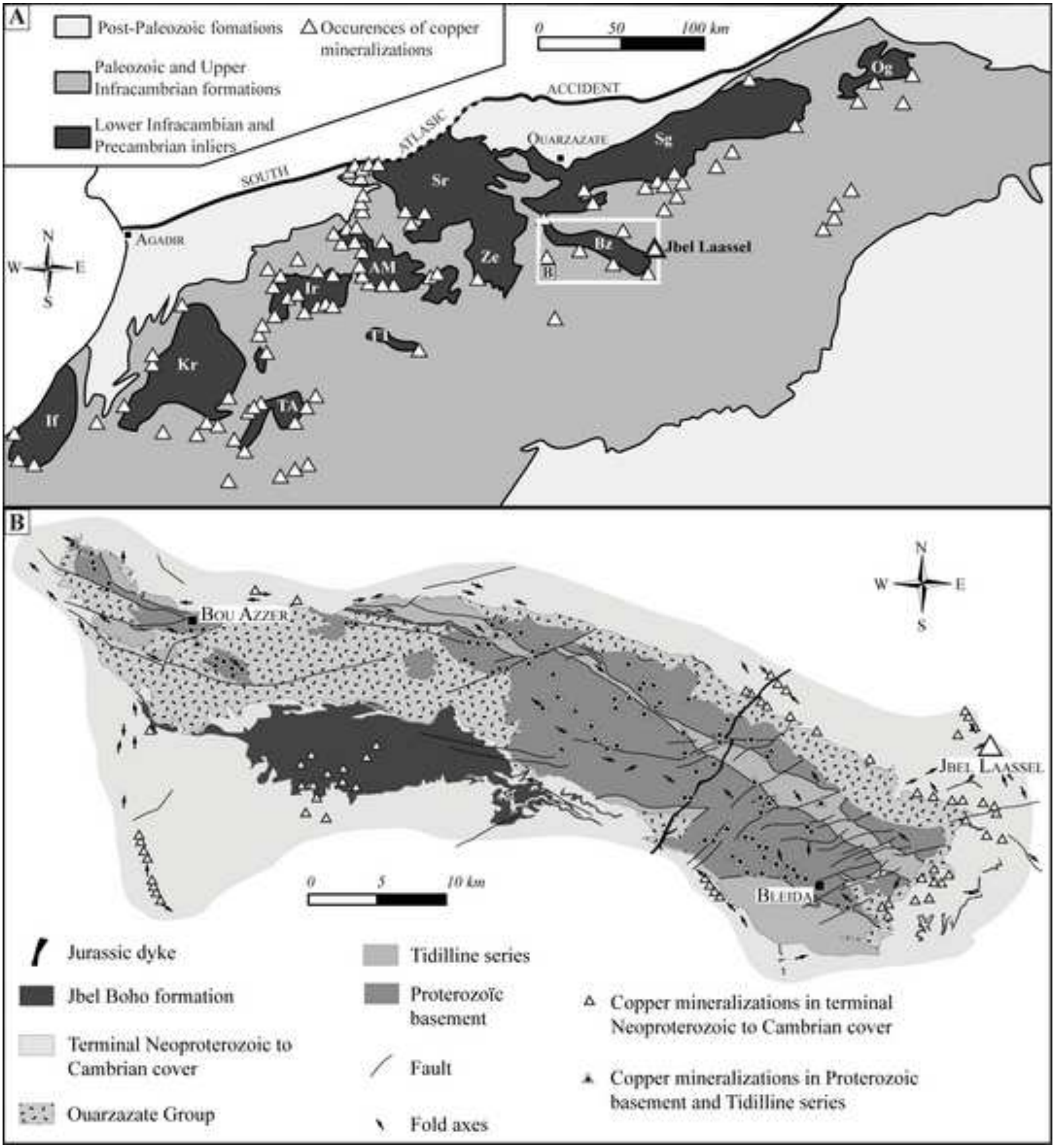

Figure 2

ACCEPTED MANUSCRIPT

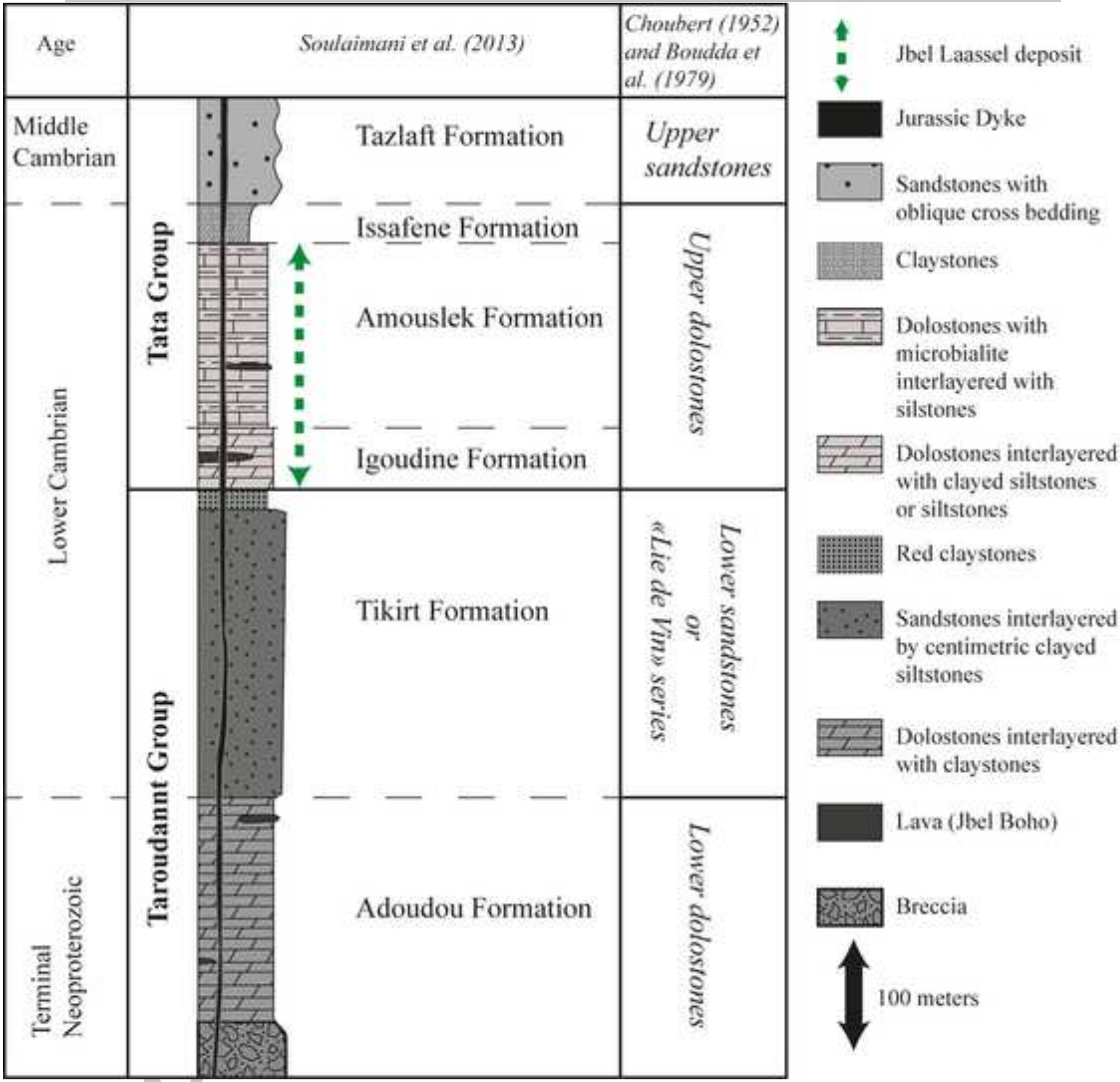

AC

Figure 3

ACCEPTED MANUSCRIPT

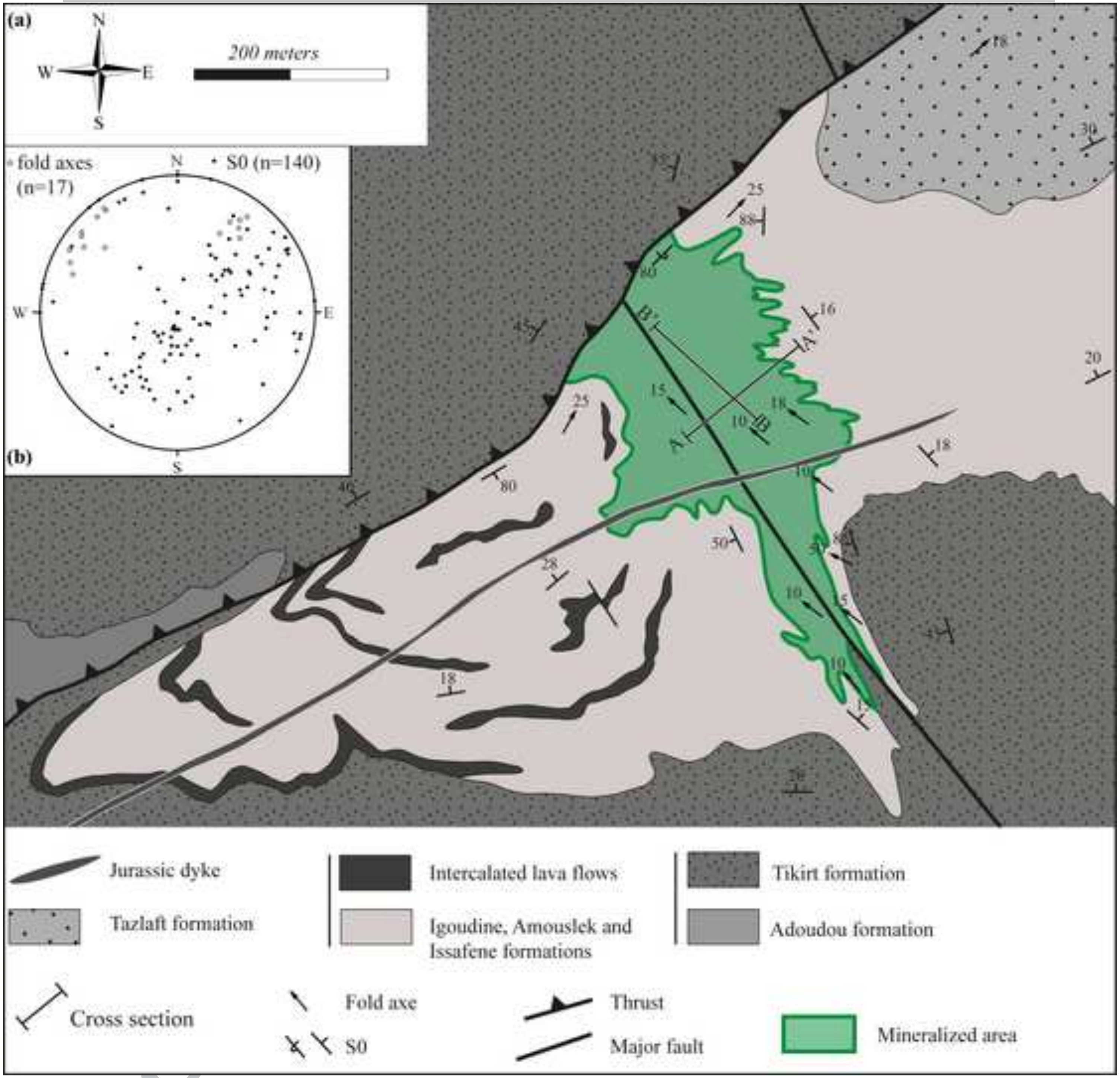

Figure 4

ACCEPTED MANUSCRIPT

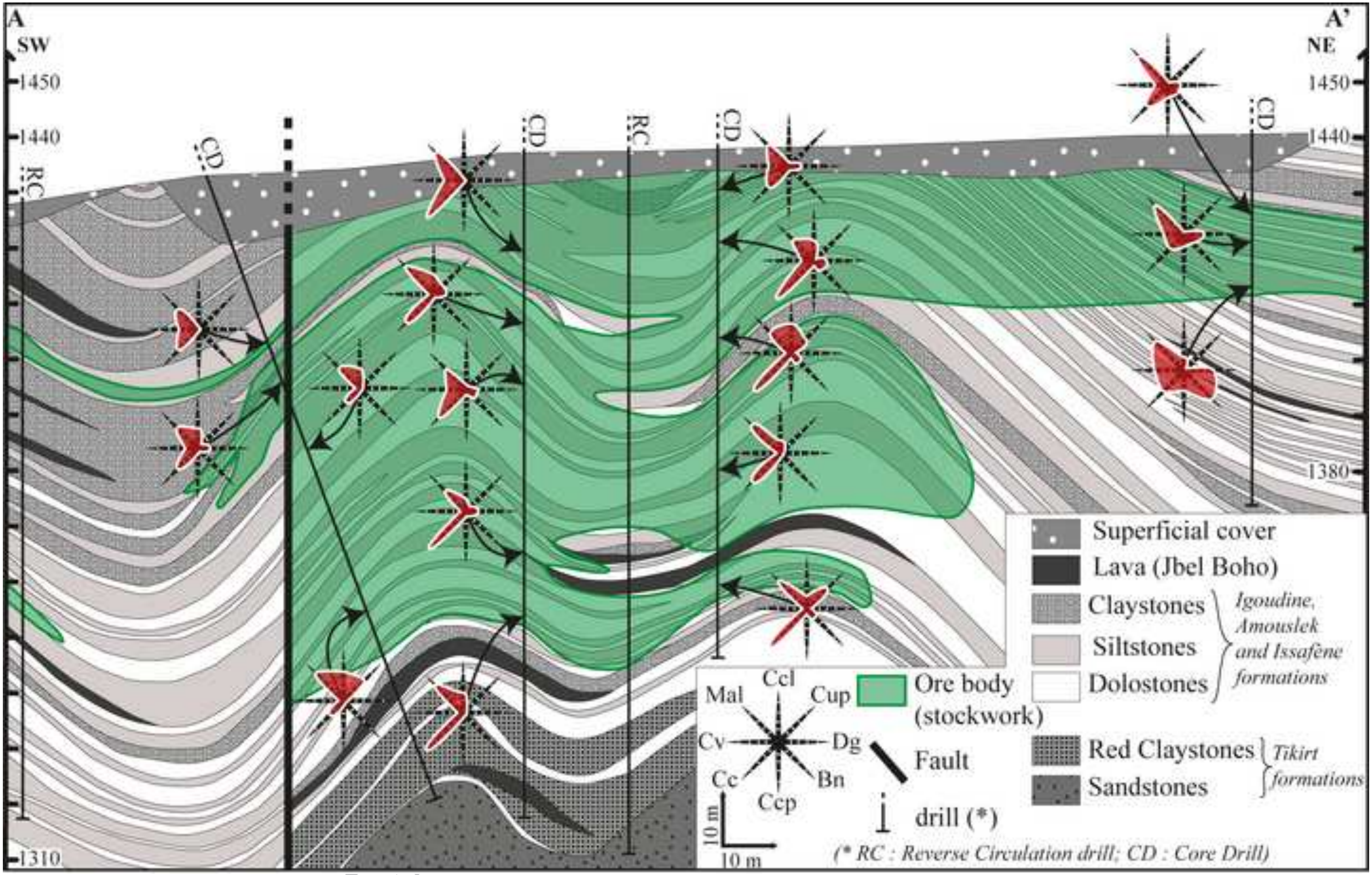

ACC

Figure 5

ACCEPTED MANUSCRIPT

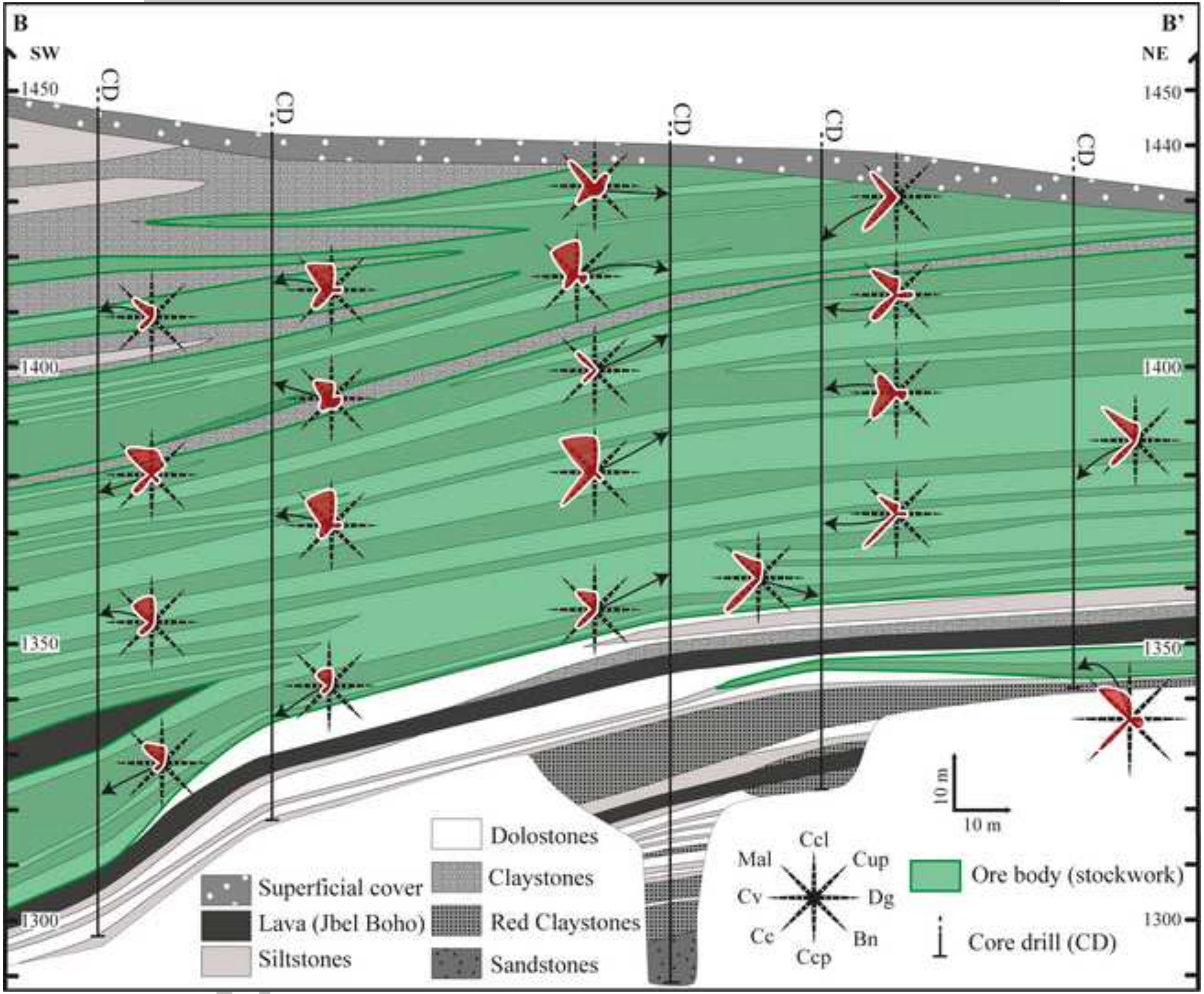

Figure 6

ACCEPTED MANUSCRIPT

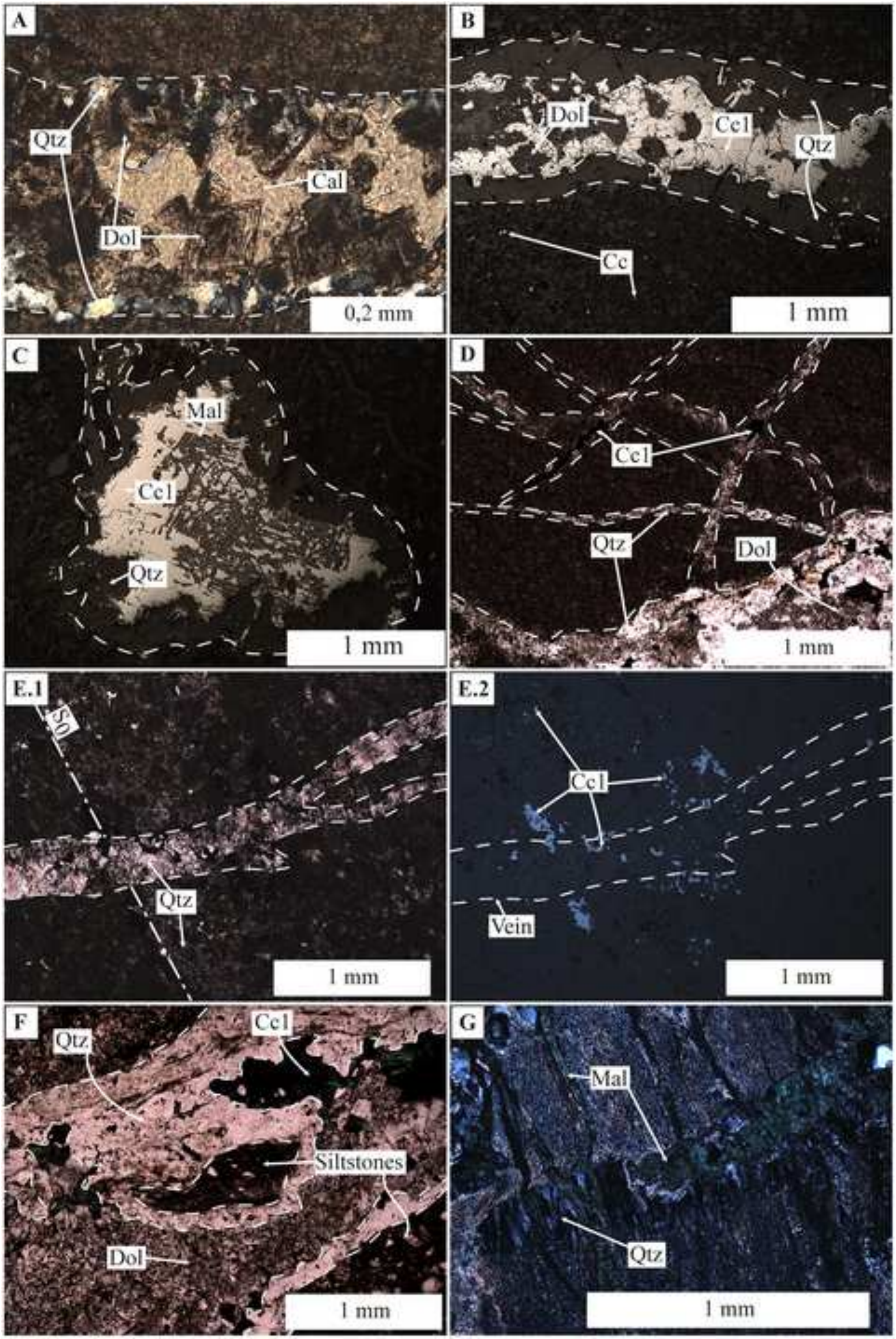

Figure 7

ACCEPTED MANUSCRIPT

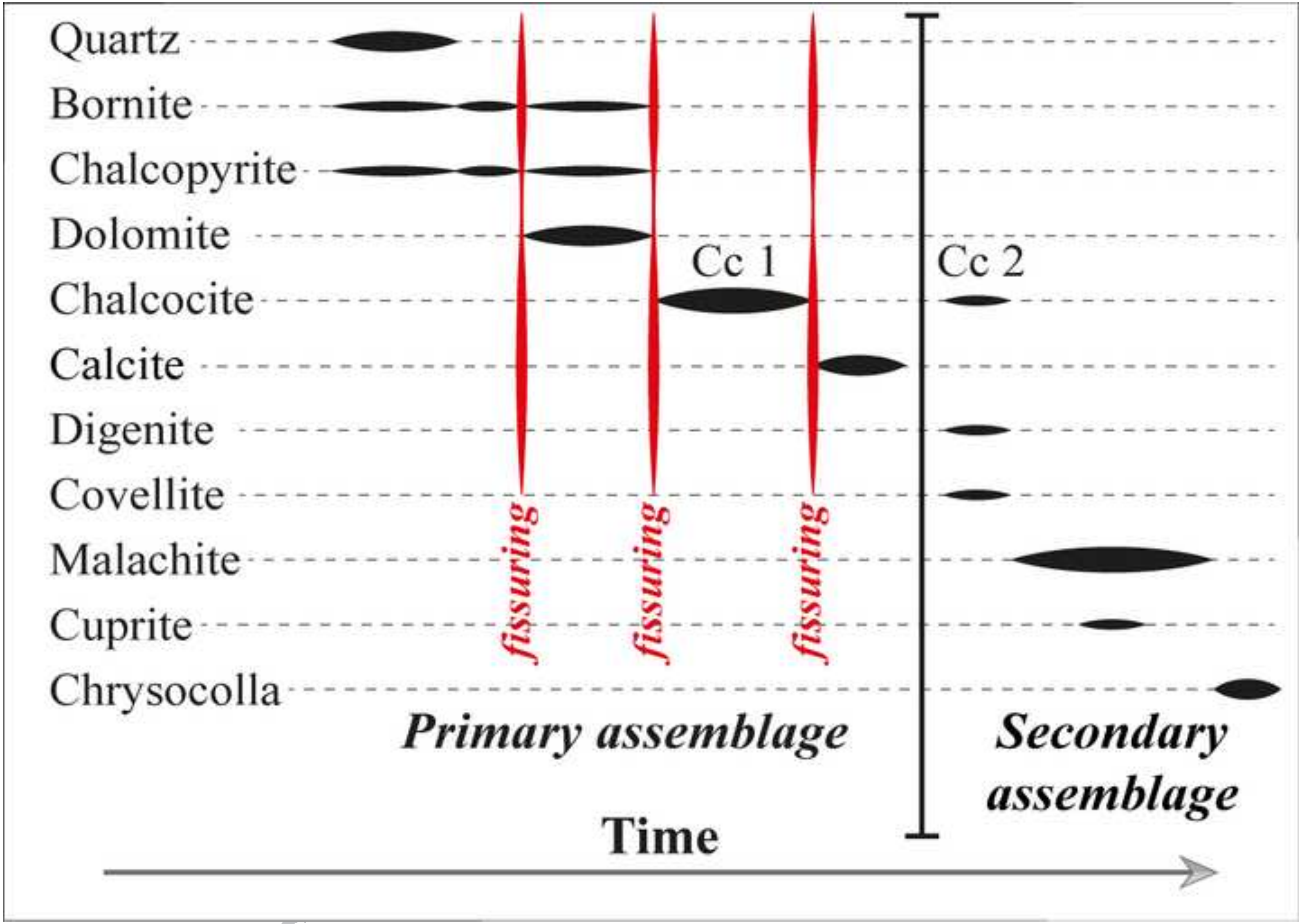

AC

Figure 8

ACCEPTED MANUSCRIPT

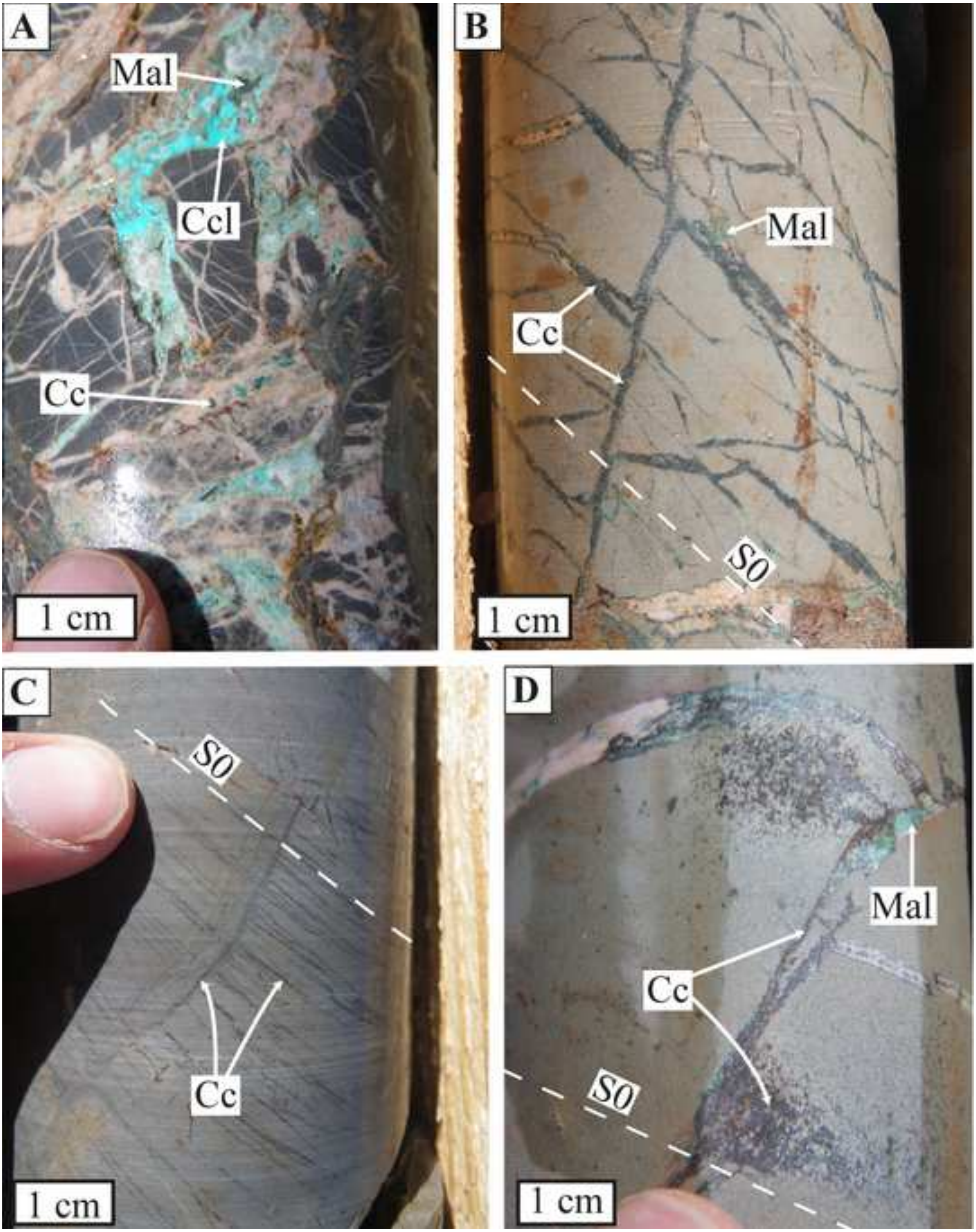

Figure 9

ACCEPTED MANUSCRIPT

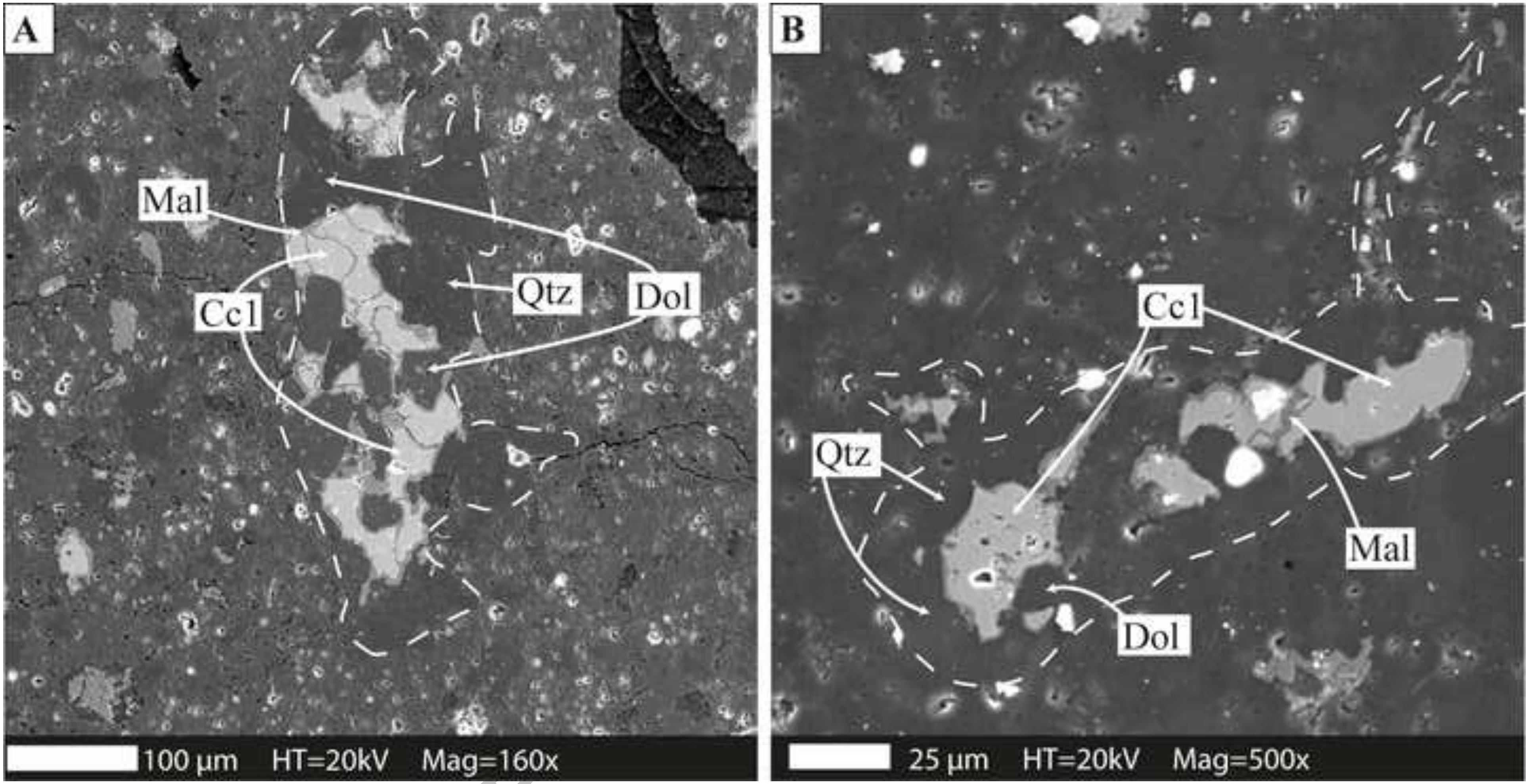

ACCEPTED

Figure 10

ACCEPTED MANUSCRIPT

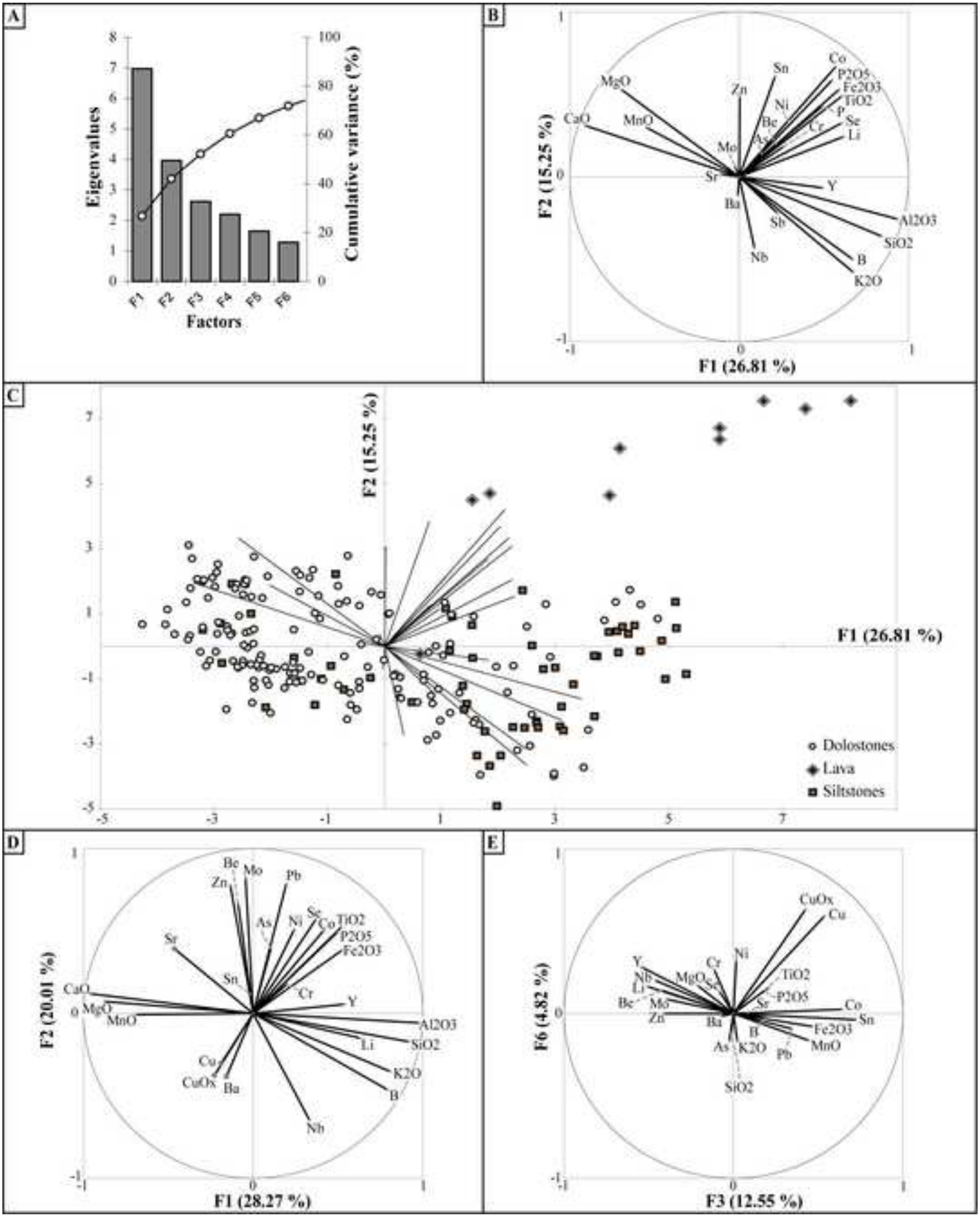

ACCEPTED MANUSCRIPT

Highlights:

- Coper mineralization occurs in a Variscan folding band in Cambrian cover.
- The mineralization appears as a stockwork with autosimilar texture.
- Results from component principal analyses don’t show relation with lithology.
- The Cu-mineralization is epigenetic, controlled by fold axis.

ACCEPTED MANUSCRIPT